Title

Additive solution deposition of multi-layered semiconducting polymer films for design of sophisticated device architectures

Journal

Journal of Materials Chemistry C, 7(4)

ISSN

2050-7526

Authors

Murrey, Tucker L
Guo, Kunping
Mulvey, Justin T
et al.

Publication Date

2019-01-24

DOI

10.1039/c8tc05652h

Peer reviewed

Journal of Materials Chemistry C

PAPER

Cite this: J. Mater. Chem. C, 2019, 7, 953

Additive solution deposition of multi-layered semiconducting polymer films for design of sophisticated device architectures†

Tucker L. Murrey,[a] Kunping Guo,[b] Justin T. Mulvey,[a] Owen A. Lee,[c] Camila Cendra,[d] Zaira I. Bedolla-Valdez,[c] Alberto Salleo,[d] Jean-Francois Moulin,[e] Kunlun Hong[f] and Adam J. Moulé*[c]

Received 9th November 2018,
Accepted 18th December 2018

DOI: 10.1039/c8tc05652h

rsc.li/materials-c

Many organic electronic devices require vertically layered structures to operate. This manuscript demonstrates an additive solution process for depositing multiple layers of semiconducting polymer (SP) films by controlling film solubility with molecular dopants. During multi-layer deposition the bottom layers are exposed to a series of solvent environments that swell the SP films. We use neutron reflectometry (NR) to quantify the film thickness change and solvent content during solvent exposure in a single poly-3-hexylthiophene (P3HT) layer. The film thickness increases by 40–80% with exposure to good solvents. Four layer thin-films composed of alternating protonated and deuterated P3HT layers were additively coated from solution. NR measurements reveal high individual layer purity and that extensive solvent soaking induces no mixing between layers. Finally, two-point conductivity measurements demonstrate that P3HT:P3HT layer interfaces have no effect on vertical conductivity. This facile process enables additive layering of mutually soluble SP films and can be used to design novel electronic device architectures.

1 Introduction

Semiconducting polymers (SPs) have received enormous attention due to low-cost scalable solution-processing, and the potential for creating light-weight flexible electronic devices.[1] Most working organic devices consist of several layers of material, each having a specific optical and/or electronic function. One universal design constraint for complicated device architectures, like organic field effect transistors (OFETs), organic photovoltaics (OPVs) and red-green-blue organic light emitting diode (OLED) displays, is that they require multiple components patterned laterally and vertically to operate.[2–4] Currently, many of these components are comprised of non-flexible inorganic materials. Typical OFETs have an organic channel and inorganic source, drain, and gate electrodes.[3,4] In order to move towards flexible all organic electronic devices, there is a need to develop high precision vertical and lateral patterning methods that are compatible with solution processing. Until now, solution processing multiple layers of SP's has been difficult because most SP's are soluble in similar solvents; coating a second layer dissolves the first layer. Thus, there is a need to develop a multilayer solution processing method that is compatible with a variety of SP's.

Unlike small molecules, polymers cannot be evaporated into multilayers.[5] One previously demonstrated method for creating multiple SP layers is by lamination. This process involves coating an SP layer onto a sacrificial substrate like poly(3,4-ethylenedioxythiophene):polystyrene sulfonate (PEDOT:PSS) or poly(sodium 4-styrenesulfonate) (PSSNa) then dissolving the substrate in water.[6,7] Water is a poor solvent for most SPs so the film is left floating on the water's surface, available to be placed onto another SP film. This method is useful for laboratory experiments but is not compatible with high-throughput scalable solution processing techniques because it forms inconsistent contact area between the two films, leading to small bi-layer areas. A more robust method for vertical patterning utilizes a stamping technique. A polydimethylsiloxane (PDMS) stamp can mechanically bind to a film, lift it off a poorly wetted substrate, and deposit the film onto a different SP film. This process enables both vertical and lateral patterning of polymer

[a] Department of Material Science and Engineering, University of California, Davis, USA
[b] Key Laboratory of Advanced Display and System Applications, Ministry of Education, Shanghai University, Shanghai, China
[c] Department of Chemical Engineering, University of California, Davis, USA. E-mail: amoule@ucdavis.edu
[d] Department of Material Science and Engineering, Stanford University, Stanford, USA
[e] REFSANS, Heinz Maier-Leibnitz Zentrum, Germany
[f] Oak Ridge National Laboratory, Oak Ridge, Tennessee, USA

† Electronic supplementary information (ESI) available. See DOI: 10.1039/c8tc05652h

films and has been used to fabricate OFETs, OPVs, and OLED displays.[8–10] Drawbacks to stamping techniques include mechanical damage, structural imperfections, and incompatibility with high throughput coating.[11]

The Moulé group recently demonstrated a patterning technique that enables lateral patterning of SPs and dopants in thin films, called dopant induced solubility control (DISC).[12,13] For DISC patterning, molecular p-type dopants like 2,3,5,6-tetrafluoro-7,7,8,8-tetracyanoquinodimethane (F4TCNQ) are sequentially introduced into a SP film using an orthogonal solvent. For example, a poly(3-hexylthiophene-2,5-diyl) (P3HT) film can be deposited from chlorobenzene (CB) then sequentially doped from a poor solvent for the polymer, such as acetonitrile (AN).[14,15] The choice of orthogonal solvent can be optimized by the degree to which it swells the polymer film. The solvent must swell the polymer to allow the dopant to diffuse through the entire film. Under specific processing conditions, P3HT/F4TCNQ systems form charge transfer (CT) states.[16] However, in the P3HT/F4TCNQ samples explored in this manuscript the dopants undergo integer charge transfer with the polymer leaving a dopant anion and a cationic hole state on the polymer.[15,17] The doped polymer is rendered insoluble by the charged states[12] and can be patterned laterally by exciting a photoinduced reaction between the F4TCNQ and tetrahydrofuran (THF).[18] While submersed in THF, the dedoped polymer dissolves into the solvent leaving a negative pattern in the film with the smallest feature size on the order of the patterning wavelength.[13,19] Since the doped polymer is insoluble and stable in solution over days, DISC patterning can easily be adapted to other coating methods, like blade or roll coating. Here we demonstrate that DISC processing steps can also be used to create a multi-layer SP film with facile solution deposition from common solvents. In order to validate this technique for creating sophisticated layered device architectures, it is critical to quantify whether sequential solvent processing steps introduce mixing between layers.

Fig. 1 shows a schematic of the additive solution processing method demonstrated here. In step (1) a multi-layer stack of N p-doped P3HT layers has already been deposited. Next, a layer of P3HT is coated on top from a good solvent for P3HT. For this study we exclusively spin coated the P3HT from CB. In step (2) the addition of P3HT solution causes the preexisting doped layers to swell with solvent. Next in step (3), the solvent evaporates leaving a new undoped P3HT layer on top of the doped P3HT layer stack. In order to render the new layer insoluble, (4) a dopant, like F4TCNQ, is introduced to the film in an orthogonal solution, like AN. Presumably, the AN swells all of the polymer layers by some amount since we know that the solvent can carry a dopant several hundreds of nm into the film. Any anhydrous orthogonal solvent for P3HT will work as a carrier solvent for the dopant. Anhydrous solvents are necessary because H_2O and/or base will react with F4TCNQ and other strong electron acceptors. In previous experiments methylene chloride, cyclohexanone, and alcohols were used to introduce F4TCNQ to polymer films. (5) The orthogonal solvent evaporates leaving a multi-layer stack of $N + 1$ doped P3HT films.

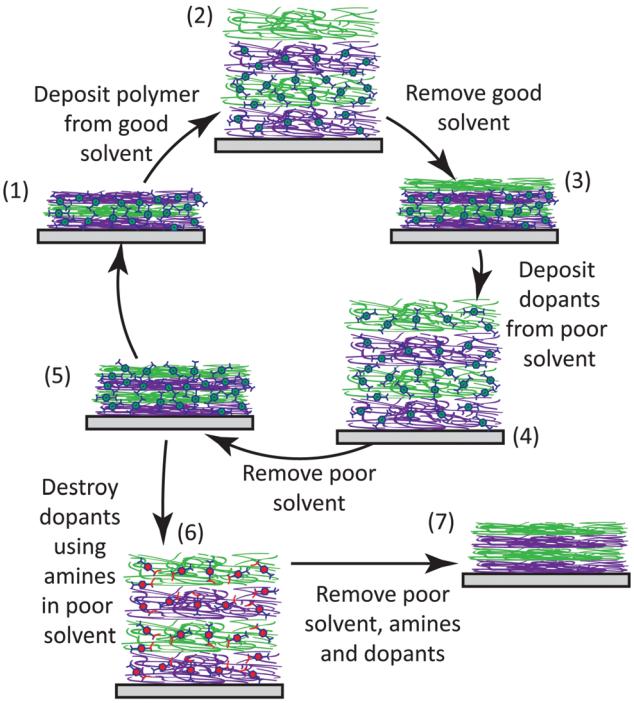

Fig. 1 Multilayer DISC patterning: this schematic displays the additive solution deposition of multiple SP layers. (1) shows an initial stack of three alternating layers of doped polymer on a substrate. In (2) a fourth undoped polymer layer is deposited from solution and (3) the solvent is removed. In (4) the top polymer layer is sequentially doped from solution and (5) the solvent is removed. Step (6) demonstrates the chemical process to dedope the polymer film and (7) depicts the final stack of neutral polymer layers.

At this point another film layer could be deposited by repeating steps 1 through 5. Alternatively, (6) all of the dopants could be deactivated by reacting F4TCNQ with a primary amine.[19] A typical dedoping solution is 10 vol% 1-butylamine and 90 vol% cyclohexanone, acetone, or AN. Again these orthogonal solvents are expected to swell all of the P3HT layers. Most of the deactivated dopant molecules are removed into the dedoping solution since the reaction product of F4TCNQ with 1-butylamine is more soluble than F4TCNQ (full dedoping takes 15 minutes).[19] (7) The final sample is a stack of $N + 1$ intrinsic P3HT layers.

Creating a four layer stack of doped films using the DISC processing steps requires that the bottom film be solvent swollen three times by a good solvent and four times by an orthogonal solvent. De-doping requires an additional solvent swelling step. It is necessary to question whether these sequential solvent processing steps result in mixing between the P3HT layers. Reptation between amorphous polymer films has been well studied, where thermal activation causes mixing between polymer layers.[20–22] However, the reptation model is only quantitative when applied to amorphous polymers with molecular weights larger than the entanglement molecular weight; regioregular P3HT is a semi-crystalline polymer. During DISC processing, the deposition solvent swells the film leaving a larger free volume for polymer reorganization and should promote polymer diffusion. At a fundamental level we investigate

the degree of swelling in P3HT and doped P3HT films when exposed to good and poor solvents in order to quantify a change in free volume. At a practical level, we investigate if the dopants prevent polymer layers from mixing during multiple solution processing steps.

2 Experimental

2.1 Materials

For neutron reflectometry (NR) and grazing incidence wide-angle X-ray scattering (GIWAXS) measurements, P3HT (M_n = 54–75 kDa, 99.995% trace metals basis, >98% Regioregularity) was purchased from Sigma Aldrich. F4TCNQ was purchased from TCI America. Fully deuterated P3HT (dP3HT) (M_n = 14.2 kDa, PDI = 1.17) was synthesized at the Center for Nanophase Materials Sciences (CNMS). Deuterated chlorobenzene (d-CB) and deuterated acetonitrile (d-AN) were purchased from Sigma Aldrich. For conductivity measurements P3HT (MW = 85–100 kDa, 99.995% trace metals basis, >90% Regioregularity) was purchased from Sigma Aldrich.

2.2 Thin film fabrication, profilometer, and UV-Vis measurements

For NR measurements, a single P3HT film and a multi-layered P3HT film were fabricated on 4 inch Si wafers. The substrates were cleaned in a series of 45 minute ultrasonic baths in acetone, 10% mucasol:DI water, and DI water before being blown dry with nitrogen and UV-ozone treated for 20 min. All spin coating occurred in a nitrogen glove box (<5 ppm H_2O, O_2). The single P3HT film was spin coated from a 20 mg mL^{-1} solution in CB at 1000 rpm for 60 seconds. The film was sequentially swollen with d-AN vapor and d-CB vapor during NR collection. The film was then doped with F4TCNQ by dipping in a 0.1 mg mL^{-1} F4TCNQ/AN solution for 10 seconds. The film was again sequentially swollen with d-AN and d-CB vapor during NR collection. Between each vapor swelling step the film was put under vacuum for 5 min. to remove excess solvent.

The four layer film was prepared with alternating deuterated P3HT (d-P3HT) and protonated P3HT layers. All four layers were spin coated at 1000 rpm for 3 s then 100 rpm for 60 s. The layers were deposited from the following CB solutions listed in the order of deposition 14 mg mL^{-1} d-P3HT, 7.25 mg mL^{-1} P3HT, 12 mg mL^{-1} d-P3HT, 6.5 mg mL^{-1} P3HT. Between each P3HT layer deposition the top layer was doped by covering the film stack with a 0.1 mg mL^{-1} solution of F4TCNQ in AN for 10 seconds before spinning off the excess solution at 3000 rpm for 30 s. The excess F4TCNQ deposits on the polymer/air interface were removed by spin coating pure AN solvent at 3000 rpm for 30 s. After the first NR was collected the four layer film was soaked in a CB bath at room temperature for 4 hours before vacuuming off excess solvent for 5 min. Preliminary thickness measurements of films deposited from these sample conditions were made using a Veeco Dektak 150 Profilometer (Table S1, ESI†). UV-Vis measurements were taken of P3HT and doped P3HT films during exposure to solvent vapor (Fig. S1, ESI†) on a Perkin Elmer Lambda 750 Spectrometer.

For GIWAXS measurements, two 300 nm P3HT films were spin coated at 1000 rpm for 3 seconds then 100 rpm for 60 seconds onto one inch native oxide silicon substrates from a 25 mg mL^{-1} solution in CB. One film was sequentially doped by covering the film with a 0.1 mg mL^{-1} solution of F4TCNQ in AN for 10 seconds before spinning off the excess solution at 3000 rpm for 30 seconds then chemically dedoped by soaking in butylamine : acetone (1 : 10 vol%) solution for 15 min.

2.3 Neutron reflectometry

The NR measurements were carried out using the REFSANS beamline at the reactor Heinz Maier-Leibnitz (FRM II).[23] This instrument makes use of a double chopper system which allows for time of flight (TOF) measurements. The collimation length and sample-detector distances were 8680 mm and 5827 mm respectively. Measurements were collected at the following two incident angles 0.6° and 1.8°. Reflectivity is measured as a function of momentum change perpendicular to the surface, $Q_z = \frac{4\pi}{\lambda}\sin\theta$, where λ is the neutron wavelength. Instrument resolution was $\frac{dQ}{Q} = 0.0335$. Reflectivity was fit with a genetic algorithm using Igor based MOTOFIT, in which the reflectivity profile is calculated with the Abeles matrix method. The scattering length densities of the bulk materials are shown in Table S2 (ESI†).

2.4 Grazing incidence wide-angle X-ray scattering

GIWAXS measurements were carried out at the Stanford Synchrotron Radiation Lightsource (SSRL) on beam line 11-3 using an area detector (Rayonix MAR-225) and incident energy of 12.73 keV. The incidence angle (0.1°) was larger than the critical angle, ensuring that we sampled the full depth of the film. A sample-detector distance of 314.99 mm was chosen and calibrated using a LaB6 polycrystalline standard. All measurements were performed under a Helium environment to minimize air scattering and beam damage to samples. Raw data was normalized by monitor counts and thickness. Data was reduced and analyzed using a combination of Nika 1D SAXS[24] and WAXStools software packages in Igor Pro.[25] Scattering data are presented in terms of scattering vector $Q = \frac{4\pi}{\lambda}\sin\theta$, where θ is half the scattering angle and λ is the wavelength of incident X-rays. The terms Q_{xy} and Q_z denote the component of scattering vector in-plane and out-of-plane with the substrate, respectively.

2.5 Conductivity measurements

Two-point vertical conductivity measurements were performed in the dark under nitrogen (<5 ppm H_2O, O_2) using a Keithley 2420 source-meter. Film device geometry is shown in Fig. S4 (ESI†). Electrode area was 19.635 mm^2.

3 Results and discussion

To elucidate the changes that may occur during subsequent solvent exposure steps we used NR[23] to study a single P3HT thin film exposed to a series of saturated d-CB and d-AN vapor environments, before and after sequentially doping the film to 7 mol% with 0.1 mg mL^{-1} F4TCNQ/AN. Deuterated solvents were used to increase the scattering length density (SLD) contrast between the polymer and solvent. Analysis of NR data allows determination of the film thickness and SLD.[26] A volume balance (eqn (S1)–(S4), ESI†) can be applied to the measured SLD to determine the volume fraction of solvent in the film (Table 1). Fig. 2(a) illustrates the series of processing steps performed on the same P3HT film. Fig. 2(b) reveals the q-dependence of the scattering intensity from the film for each of the processing conditions (offset vertically). Fig. 2(c) shows the corresponding vertical SLD profiles obtained from fits to the NR data.

Table 1 Solvent volume fraction and percent film thickness increase obtained from NR fits

Film	Solvent	$\phi_{solvent}$	ΔT (%)
P3HT	d-AN	0.02 ± 0.01	1.1 ± 1
	d-CB	0.49 ± 0.02	81.4 ± 6.4
Doped P3HT	d-AN	0.06 ± 0.01	14.3 ± 2.5
	d-CB	0.39 ± 0.01	43.4 ± 4.6

Step (1) begins with a neutral P3HT film spin coated onto an Si:SiO$_2$ substrate from a CB solution. In (2), the neutral P3HT film was exposed to a saturated vapor of d-AN. As mentioned above d-AN is an orthogonal solvent for P3HT; the film thickness only increases 1.1 ± 1.0% when exposed to d-AN vapor. The small increase in SLD corresponds to 2 ± 1 vol% of d-AN penetrating the free space in the amorphous regions of the polymer film. This exhibits a necessary requirement for sequential doping: the carrier solvent for the dopant must swell the polymer enough to promote diffusion of the dopant through the entirety of the film. However, if mixing between the solvent and the polymer is too thermodynamically favorable it will result in unwanted changes to film morphology or dissolution. In (3), the neutral P3HT film was exposed to a saturated vapor of d-CB causing the film to swell significantly, with d-CB occupying 49 ± 2 vol% of the film and causing an 81.4 ± 6.4% thickness increase. Since d-CB is a good solvent for P3HT, the film swells as much as entanglement allows. The volume percent of d-CB in the film decreases near the substrate due to attractive substrate–polymer interactions.[27] Between each solvent swelling step the film was placed under vacuum to remove residual solvent.

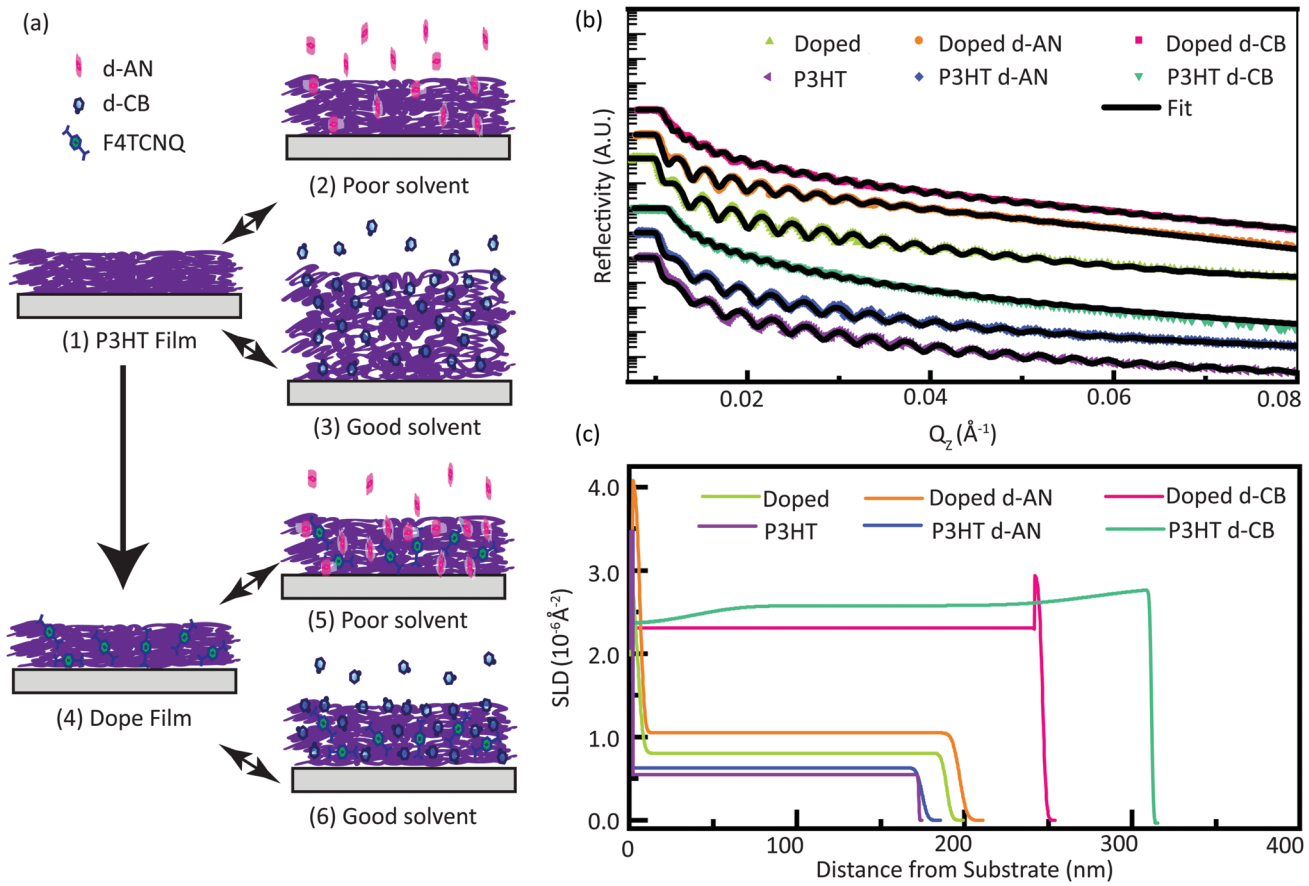

Fig. 2 (a) Processing steps for the single P3HT film sequentially swollen with saturated d-AN vapor and d-CB vapor, then doped with F4TCNQ and sequentially swollen with d-AN vapor and d-CB vapor. (b) Neutron reflectivity data and best fit (c) vertical scattering length density profiles from NR fits.

After the first three NR measurements, the same P3HT film was sequentially doped with F4TCNQ by dipping in a 0.1 mg mL^{-1} solution of F4TCNQ/AN (4). Due to technical challenges during collection, the NR of the doped film was collected after the swelling experiments with the doped film. However, since there was no heating or removal of solvent other than by evaporation, we are confident that the dopant concentration is identical in all three experiments. The doped film has higher SLD due to the scattering from the nitrogen and fluorine atoms on the F4TCNQ. The doped film swelled 43.4 ± 4.6% during d-CB vapor exposure and did not collapse back to its initial thickness after exposure, remaining 9.9 ± 2.2% thicker than the undoped film. This increased layer thickness after solvent exposure only occurs in the presence of the dopant. The original neutral P3HT film was deposited from CB. Further exposure of an undoped P3HT film to CB does not permanently affect film thickness. Our group previously showed that sequential addition of F4TCNQ to a P3HT film results in addition of dopants to amorphous domains. Only with secondary exposure to CB do the dopants intercalate to crystalline domains causing the π–π stacking dimension to shrink from 0.39 nm to 0.38 nm.[14] More recently, Chew *et al.* showed that adding F4TCNQ to P3HT *via* sequential doping results in significant stiffening of tie-chains between crystalline domains.[28] These results together suggest that when the doped film is solvent swollen, F4TCNQ redistributes in the film and stiffens sections of the P3HT chains. When the solvent evaporates, the film is less dense due to inefficient packing of these stiffer chain sections. The sharp increase in SLD near the silicon interface corresponds to the formation of a F4TCNQ mono-layer. Several studies have shown that F4TCNQ p-type dopes silicon.[29,30] In (5), the doped P3HT film was exposed to a saturated vapor of d-AN. When exposed to d-AN vapor the doped film swells 14.3 ± 2.5% and contains 6 ± 1 vol% d-AN. In (6), the doped P3HT film was exposed to a saturated vapor of d-CB. When exposed to d-CB vapor the doped film swelled 43.4 ± 4.6% containing 39 ± 1 vol% d-CB. This is 21% thinner than the neutral d-CB swollen P3HT film.

The Hansen solubility parameters for CB and AN representing dispersion, polar, and hydrogen bonding forces are (δ_d = 9.28, δ_p = 2.1, δ_h = 1.0) and (δ_d = 7.5, δ_p = 8.8, δ_h = 3.0) respectively.[31] AN has higher polar bonding forces than CB. Since F4TCNQ forms cation/anion pairs with P3HT increasing the polarity of select regions of the film, it is reasonable to consider that the doped film would swell more in AN. Likewise, increasing the polarity of the film should reduce miscibility with CB.

To demonstrate our multilayer deposition process, we created a doped four-layer P3HT film stack with alternating deuterated (d-P3HT) and protonated (p-P3HT) layers. The layer thicknesses were characterized using NR. Fig. 3(a) presents the *q*-dependence of the scattering intensity and Fig. 3(b) displays the vertical SLD profiles obtained from the fits. The SLD profile reveals four distinct layers that are purely d-P3HT or p-P3HT. The average layer interface width is 7.58 ± 0.65 nm. Although the bottom d-P3HT:p-P3HT interface was solvent swollen more times than subsequent interfaces (see Fig. 1) there is no additional mixing.

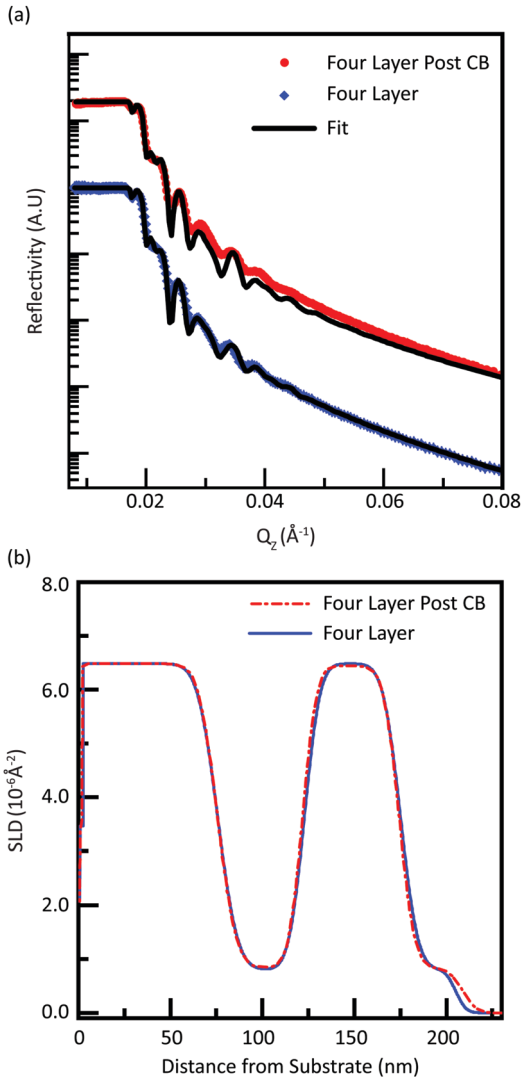

Fig. 3 (a) Neutron reflectivity from a four layered doped P3HT film with alternating deuterated and protonated layers before and after soaking in CB bath for 4 hours, (b) vertical scattering length density profiles from NR fits.

The overall interface roughness is elevated compared to previous bi-layer experiments using polystyrene because P3HT is semi-crystalline.[32] Also, the roughness is measured over a 8–10 cm strip in the film; any thickness change over several cm increases the apparent interface roughness over the measured length scale. We were not able to optimize the deposition conditions to minimize the interface roughness due to a limited supply of d-P3HT. Nevertheless, the data clearly shows pure layered films with sharp interfaces and constant roughness with respect to the number of solution processing steps.

After the first NR measurement, the four-layer film was soaked in a bath of liquid CB at room temperature for 4 hours. The sample was then removed from the bath, dried under vacuum, and a second NR measurement was performed. The top doped P3HT layer thickness increased after soaking because, unlike the bottom three layers, it had not been exposed to CB since it was deposited. The presence of F4TCNQ

in the layer prevents the film from collapsing back to its original thickness, as was shown in the solvent swelling experiment in Fig. 2(c). The data also shows that solvent soaking did not induce mixing between the layers; the layer thicknesses, purity of the layers, and interface widths remain constant after soaking in CB. As shown above, a doped P3HT film swollen with d-CB has a volume increase of 43.4 ± 4.6%. Assuming the entirety of this increase adds to the free volume around the polymer chains, we expected to observe a sharp increase in diffusion at the layer interfaces, even without a temperature increase. Without considering the effects of dopants, polymer diffusion and solubility are known to decrease with increasing molecular weight.[20,21,33] Since our d-P3HT has a lower molecular weight of 14.4 kDa, we expected layer mixing to result from diffusion of the d-P3HT into the higher molecular weight p-P3HT (~65 kDa). However, there is no observable mixing between layers during the explored timescale. All things considered, the presence of the dopant:

1. Prevents the film from swelling as much as the undoped polymer film.

2. Prevents mixing at d-P3HT:p-P3HT interfaces during solution deposition.

3. Prevents the film from collapsing back to its original thickness after swelling with a good solvent.

Since the ultimate goal of this multilayer deposition process is to demonstrate its viability for creating sophisticated layered device architectures, we explore whether the presence of polymer:polymer interfaces significantly changes the electronic properties of the film. We prepared a series of single, double, and quadruple layer p-P3HT films with a 200 nm total thickness. We then performed two-point conductivity measurements vertically through the film to explore whether the polymer: polymer interfaces have any effect on the vertical conductivity of a multi-layer film. The device architecture is located in Fig. S4 and *I–V* curves are located in Fig. S5–S10 (ESI†). We compare samples that are doped to samples in which the F4TCNQ was removed using a reaction with butylamine.[19] We further characterized the morphology of P3HT and chemically dedoped P3HT films using GIWAXS. (Table 2 and Fig. S2, S3, ESI†). The lattice spacings extracted from fitting the diffraction peak positions of the lamellar (200) and π–π stacking (010) spacings show that the film microstructure is not affected by chemical dedoping. For the π–π direction, the coherence length can be calculated using peak widths and the Scherrer equation. Chemical dedoping produces a small decrease in the coherence length. Fig. 4 shows the conductivity as a function of the number of p-P3HT layers. The error bars were generated by multiple measurements of several samples with small thickness variations.

Table 2 P3HT and dedoped P3HT π–π stacking distance and lamellar spacing from grazing incidence wide-angle X-ray scattering

Sample	π–π stacking distance (Å)	Coherence length (nm)	Lamellar spacing (Å)
P3HT	3.86 ± 0.01	8.0 ± 0.1	16.29 ± 0.01
Dedoped P3HT	3.85 ± 0.01	7.3 ± 0.1	16.26 ± 0.01

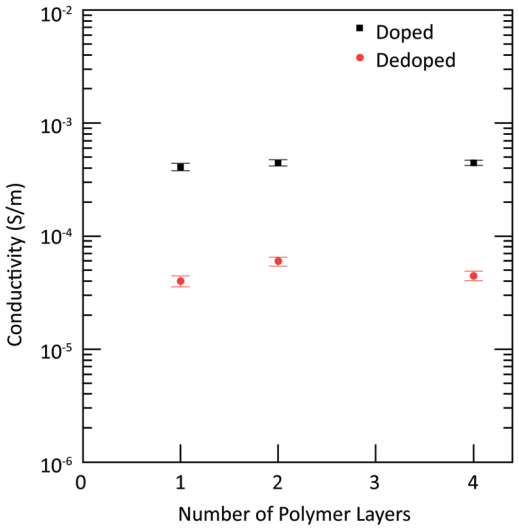

Fig. 4 Two-point vertical conductivity measurements of doped and dedoped single, double, and quadruple P3HT layer devices.

For both doped and dedoped samples, there is no statistically significant change in the out-of plane conductivity as a function of the number of layer interfaces. The overall conductivity of the dedoped P3HT samples is consistent with literature values for neutral P3HT.[34] However our doped film conductivity is a few orders of magnitude lower than previous observations.[14,15] Zuo *et al.* obtained high in-plane conductivities on the order of 10^2 S m^{-1} from sequentially deposited P3HT:F4TCNQ films.[35] This discrepancy is likely the result of using different measurement techniques. Two-point conductivity measurements are susceptible to high contact resistance.[36] Our NR data shows that F4TCNQ forms a monolayer on an $Si:SiO_2$ substrate. F4TCNQ is known to form a surface layer on gold that increases the work function and thus the extraction barrier for holes from doped P3HT.[37] A further complication is that F4TCNQ undergoes significant drift in P3HT resulting in a non-linear current voltage characteristic.[38] Here we used low voltages (−0.01 to 0.01 V) to minimize any contribution to resistivity from dopant drift. Regardless, the data shows identical conductivity for all three doped and all three de-doped samples. We can safely conclude that the presence of polymer:polymer interfaces in a vertical multi-layer stack makes no significant contribution to vertical conductivity.

4 Conclusion

This manuscript demonstrates a novel solution deposition process for multi-layered SP films. Each sequential solution processing step swells the polymer film and is quantified with NR. Doped P3HT swells to >40% in a good solvent but does not dissolve. We fabricated a four layer stack of alternating deuterated and protonated P3HT layers using the DISC method. NR shows that all four layers are pure with negligible mixing between sequential layers. Solvent soaking in CB for 4 hours swells the layer stack but does not result in any

additional mixing between layers. This shows that sequential solvent processing does not induce layer mixing and that DISC patterning is a viable technique for roll-to-roll compatible coating processes including dip coating, blade coating, spin coating, and/or ink jet printing. Finally, we measured the vertical conductivity as a function of the number of P3HT:P3HT layer interfaces and found that interfaces did not affect the vertical conductivity. We want to emphasize that this simple additive deposition technique facilitates the design of novel layered architectures by allowing the sequential deposition of mutually soluble SP films. With chemical dedoping one may create doped or dedoped layered architectures for various electronic applications. We expect this technique to be compatible with other SP/dopant systems and may one day be used to design multi-layered all-organic electronic devices.

Conflicts of interest

There are no conficts of interest to declare.

Acknowledgements

This project was supported by the U.S. Department of Energy, Office of Basic Energy Sciences, Division of Materials Sciences and Engineering, under Award No. DE-SC0010419. Thanks to the Jülich Centre for Neutron Science at Heinz Maier-Leibnitz Zentrum in Garching, Germany for Neutron Reflectometry measurement time and salary for J. F. M. The synthesis of d-P3HT was carried out at the Center for Nanophase Materials Sciences, which is a DOE Office of Science User Facility. X-ray diffraction measurement were carried out at the Stanford Synchrotron Radiation Lightsource, a national user facility operated by Stanford University on behalf of the U.S. Department of Energy, Office of Basic Energy Sciences. The X-ray measurements performed by C. C. and A. S. were supported by the National Science Foundation award No. 1636385. Z. I. B-V. thanks SENER-CONACyT project No. 291145 for postdoctoral support. Thanks to the China Scholarship Council No. 201706890052 for support for K. G. and to the Wasson Family thesis program for support for J. T. M.

Notes and references

1 C. Wang, H. Dong, W. Hu, Y. Liu and D. Zhu, *Chem. Rev.*, 2012, **112**, 2208–2267.
2 F. Guo, A. Karl, Q.-F. Xue, K. C. Tam, K. Forberich and C. J. Brabec, *Light: Sci. Appl.*, 2017, **6**, e17094.
3 B. Lüssem, C.-M. Keum, D. Kasemann, B. Naab, Z. Bao and K. Leo, *Chem. Rev.*, 2016, **116**, 13714–13751.
4 H. Sirringhaus, *Adv. Mater.*, 2014, **26**, 1319–1335.
5 U. Heider, *OLED and Merck's respective position (A Deep Dive into Merck's LC & OLED Business)*, Merck technical report, 2013.
6 A. Karim, G. P. Felcher and T. P. Russell, *Macromolecules*, 1994, **27**, 6973–6979.
7 K. Nakano and K. Tajima, *Adv. Mater.*, 2016, **29**, 1603269.
8 M. Ikawa, T. Yamada, H. Matsui, H. Minemawari, J. Tsutsumi, Y. Horii, M. Chikamatsu, R. Azumi, R. Kumai and T. Hasegawa, *Nat. Commun.*, 2012, **3**, 1176.
9 A. L. Shu, A. Dai, H. Wang, Y.-L. Loo and A. Kahn, *Org. Electron.*, 2013, **14**, 149–155.
10 J. Li, L. Xu, C. W. Tang and A. A. Shestopalov, *ACS Appl. Mater. Interfaces*, 2016, **8**, 16809–16815.
11 A. C. Arias, J. D. MacKenzie, I. McCulloch, J. Rivnay and A. Salleo, *Chem. Rev.*, 2010, **110**, 3–24.
12 I. E. Jacobs, J. Li, S. L. Berg, D. J. Bilsky, B. T. Rotondo, M. P. Augustine, P. Stroeve and A. J. Moule, *ACS Nano*, 2015, **9**, 1905–1912.
13 I. E. Jacobs, E. W. Aasen, D. Nowak, J. Li, W. Morrison, J. D. Roehling, M. P. Augustine and A. J. Moulé, *Adv. Mater.*, 2017, **29**, 1603221.
14 I. E. Jacobs, E. W. Aasen, J. L. Oliveira, T. N. Fonseca, J. D. Roehling, J. Li, G. Zhang, M. P. Augustine, M. Mascal and A. J. Moulé, *J. Mater. Chem. C*, 2016, **4**, 3454–3466.
15 D. T. Duong, C. Wang, E. Antono, M. F. Toney and A. Salleo, *Org. Electron.*, 2013, **14**, 1330–1336.
16 I. E. Jacobs, C. Cendra, T. F. Harrelson, Z. I. Bedolla Valdez, R. Faller, A. Salleo and A. J. Moulé, *Mater. Horiz.*, 2018, **5**, 655–660.
17 J. Gao, J. D. Roehling, Y. Li, H. Guo, A. J. Moulé and J. K. Grey, *J. Mater. Chem. C*, 2013, **1**, 5638–5646.
18 J. Fuzell, I. E. Jacobs, A. Ackling, T. F. Harrelson, D. M. Huang, D. S. Larsen and A. J. Moule, *J. Phys. Chem. Lett.*, 2016, **7**, 4297–4303.
19 I. E. Jacobs, F. Wang, N. Hafezi, C. Medina-Plaza, T. F. Harrelson, J. Li, M. P. Augustine, M. Mascal and A. J. Moulé, *Chem. Mater.*, 2017, **29**, 832–841.
20 T. P. Russell, V. R. Deline, W. D. Dozier, G. P. Felcher, G. Agrawal, R. P. Wool and J. W. Mays, *Nature*, 1993, **365**, 235.
21 P. G. de Gennes, *J. Chem. Phys.*, 1971, **55**, 572–579.
22 M. Doi and S. F. Edwards, *J. Chem. Soc., Faraday Trans. 2*, 1978, **74**, 1818–1832.
23 M. H. Heinz Maier-Leibnitz Zentrum and J.-F. Moulin, *Journal of large-scale research facilities*, 2015, **1**, A9.
24 J. Ilavsky, *J. Appl. Crystallogr.*, 2012, **45**, 324–328.
25 S. D. Oosterhout, V. Savikhin, J. Zhang, Y. Zhang, M. A. Burgers, S. R. Marder, G. C. Bazan and M. F. Toney, *Chem. Mater.*, 2017, **29**, 3062–3069.
26 J. Penfold and R. K. Thomas, *J. Phys.: Condens. Matter*, 1990, **2**, 1369.
27 Y. Guo, X. Ma and Z. Su, *Macromolecules*, 2013, **46**, 2733–2739.
28 A. R. Chew, R. Ghosh, Z. Shang, F. C. Spano and A. Salleo, *J. Phys. Lett.*, 2017, **8**, 4974–4980.
29 S. Yoshimoto, M. Furuhashi, T. Koitaya, Y. Shiozawa, K. Fujimaki, Y. Harada, K. Mukai and J. Yoshinobu, *J. Appl. Phys.*, 2014, **115**, 143709.
30 M. Furuhashi and J. Yoshinobu, *J. Phys. Lett.*, 2010, **1**, 1655–1659.
31 C. M. Hansen, *The three dimensional solubility parameter and solvent diffusion coefficient: Their importance in surface coating formulation*, 1967.

32 T. P. Russell, A. Karim, A. Mansour and G. P. Felcher, *Macromolecules*, 1988, **21**, 1890–1893.
33 B. A. Miller-Chou and J. L. Koenig, *Prog. Polym. Sci.*, 2003, **28**, 1223–1270.
34 V. Skrypnychuk, N. Boulanger, V. Yu, M. Hilke, S. C. B. Mannsfeld, M. F. Toney and D. R. Barbero, *Adv. Funct. Mater.*, 2014, **25**, 664–670.
35 G. Zuo, O. Andersson, H. Abdalla and M. Kemerink, *Appl. Phys. Lett.*, 2018, **112**, 083303.
36 I. Miccoli, F. Edler, H. Pfnür and C. Tegenkamp, *J. Phys.: Condens. Matter*, 2015, **27**, 223201.
37 G. M. Rangger, O. T. Hofmann, L. Romaner, G. Heimel, B. Bröker, R.-P. Blum, R. L. Johnson, N. Koch and E. Zojer, *Phys. Rev. B: Condens. Matter Mater. Phys.*, 2009, **79**, 165306.
38 L. Muller, S.-Y. Rhim, V. Sivanesan, D. Wang, S. Hietzschold, P. Reiser, E. Mankel, S. Beck, S. Barlow, S. R. Marder, A. Pucci, W. Kowalsky and R. Lovrincic, *Adv. Mater.*, 2017, **29**, 1701466.

